Inorganic Chemistry

ARTICLE

pubs.acs.org/IC

Cluster Expansion Reactions of Group 6 and 8 Metallaboranes Using Transition Metal Carbonyl Compounds of Groups 7−9

K. Geetharani,[†] Shubhankar Kumar Bose,[†] Satyanarayan Sahoo,[†] Babu Varghese,[‡] Shaikh M. Mobin,[§] and Sundargopal Ghosh*[,†]

[†]Department of Chemistry and [‡]Sophisticated Analytical Instruments Facility, Indian Institute of Technology Madras, Chennai 600 036, India

[§]National Single Crystal X-ray Diffraction Facility, Indian Institute of Technology Bombay, Mumbai 400 076, India

Supporting Information

ABSTRACT: The reinvestigation of an early synthesis of heterometallic cubane-type clusters has led to the isolation of a number of new clusters which have been characterized by spectroscopic and crystallographic techniques. The thermolysis of $[(Cp^*Mo)_2B_4H_4E_2]$ (**1**: E = S; **2**: E = Se; $Cp^* = \eta^5$-C_5Me_5) in presence of $[Fe_2(CO)_9]$ yielded cubane-type clusters $[(Cp^*Mo)_2(\mu_3\text{-}E)_2B_2H(\mu\text{-}H)\{Fe(CO)_2\}_2Fe(CO)_3]$, **4** and **5** (**4**: E = S; **5**: E = Se) together with fused clusters $[(Cp^*Mo)_2B_4H_4E_2Fe(CO)_2Fe(CO)_3]$ (**8**: E = S; **9**: E = Se). In a similar fashion, reaction of $[(Cp^*RuCO)_2B_2H_6]$, **3**, with $[Fe_2(CO)_9]$ yielded $[(Cp^*Ru)_2(\mu_3\text{-}CO)_2B_2H(\mu\text{-}H)\{Fe(CO)_2\}_2Fe(CO)_3]$, **6**, and an incomplete cubane cluster $[(\mu_3\text{-}BH)_3(Cp^*Ru)_2\{Fe(CO)_3\}_2]$, **7**. Clusters **4**−**6** can be described as heterometallic cubane clusters containing a $Fe(CO)_3$ moiety *exo*-bonded to the cubane, while **7** has an incomplete cubane $[Ru_2Fe_2B_3]$ core. The geometry of both compounds **8** and **9** consist of a bicapped octahedron $[Mo_2Fe_2B_3E]$ and a trigonal bipyramidal $[Mo_2B_2E]$ core, fused through a common three vertex $[Mo_2B]$ triangular face. In addition, thermolysis of **3** with $[Mn_2(CO)_{10}]$ permits the isolation of *arachno*-$[(Cp^*RuCO)_2B_3H_7]$, **10**. Cluster **10** constitutes a diruthenaborane analogue of 8-sep pentaborane(11) and has a structural isomeric relationship to 1,2-$[\{Cp^*Ru\}_2(CO)_2B_3H_7]$.

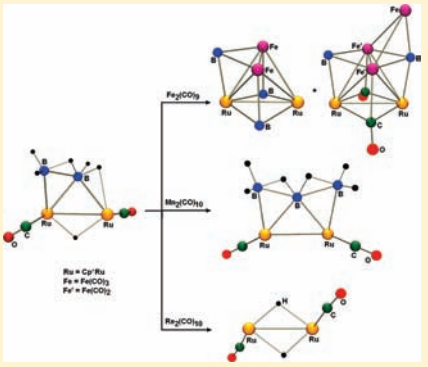

INTRODUCTION

Over time, and in the shadow of organometallic chemistry, a systematic structural chemistry for Polyboron−metal compounds developed. The development of metallaborane chemistry blossomed with the discovery of both cluster electron counting rules and the isolobal principle, that provide a solid foundation for understanding the interrelationships between structure and composition.[1] In cluster chemistry, several approaches to the construction of clusters have received much attention.[2,3] For example, (i) condensation involving monoborane reagents,[4] (ii) insertion or fragmentation involving borane or metal carbonyl fragments,[5] and (iii) intercluster fusion with two or more atoms held in common between the constituent subclusters.[6] In each case the reaction often leads to the formation of a wide range of products with different metal-to-boron ratios.[7−11]

Compounds **1**−**3**[12,13] were found to be useful precursors for the formation of cubane clusters. Thus, the chemistry was elaborated by means of cluster expansion reaction with $[Fe_2(CO)_9]$, which led to the isolation of cubane-type clusters $[(Cp^*M)_2(\mu_3\text{-}E)_2B_2H(\mu\text{-}H)\{Fe(CO)_2\}_2Fe(CO)_3]$, **4**−**6** (**4**: M = Mo, E = S; **5**: M = Mo, E = Se; **6**: M = Ru, E = CO). In addition to the cubane clusters, we have isolated an incomplete cubane-type cluster $[(\mu_3\text{-}BH)_3(Cp^*Ru)_2\{Fe(CO)_3\}_2]$, **7**, from **3** and fused clusters $[(Cp^*Mo)_2B_4H_4E_2Fe(CO)_2Fe(CO)_3]$ (**8**: E = S; **9**: E = Se) from **1** and **2**, respectively. Preliminary results have already been communicated earlier.[14] Further, the chemistry of **3** has been elaborated with $[Mn_2(CO)_{10}]$ and $[Re_2(CO)_{10}]$, which led to the isolation of *arachno*-$[(Cp^*RuCO)_2B_3H_7]$, **10** and hydrido carbonyl complex $[Cp^*Ru(CO)(\mu\text{-}H)]_2$, **11**.

RESULTS AND DISCUSSION

As shown in Scheme 1, reaction of a reddish brown solution of **1** in toluene with excess of $[Fe_2(CO)_9]$ resulted in the formation of **4** and **8**. Similarly, compound **2** on reaction with $[Fe_2(CO)_9]$ yielded **5** and **9**. Reaction of a yellow solution of **3** in presence of $[Fe_2(CO)_9]$ generated compounds **6** and **7**. Details of spectroscopic and structural characterization of **4**−**9** using IR, ^1H, ^{11}B, ^{13}C NMR, mass spectrometry, and X-ray diffraction studies follow.

Cubane Clusters 4−7. The constitution of **5** was ascertained by an X-ray diffraction study on a suitable single crystal (Figure 1). The compound crystallizes in the monoclinic space group $P2_1/c$ and displays the existence of a novel "capped cubane" cluster core. Although X-ray quality crystals of **4** have not been obtained yet, its identity is inferred by comparison to

Received: April 19, 2011
Published: May 25, 2011

Scheme 1. (a) Synthesis of 4, 5, 8, and 9; (b) Synthesis of 6, 7, 10, and Triply Bridged Heterometallic Borylene Complexes

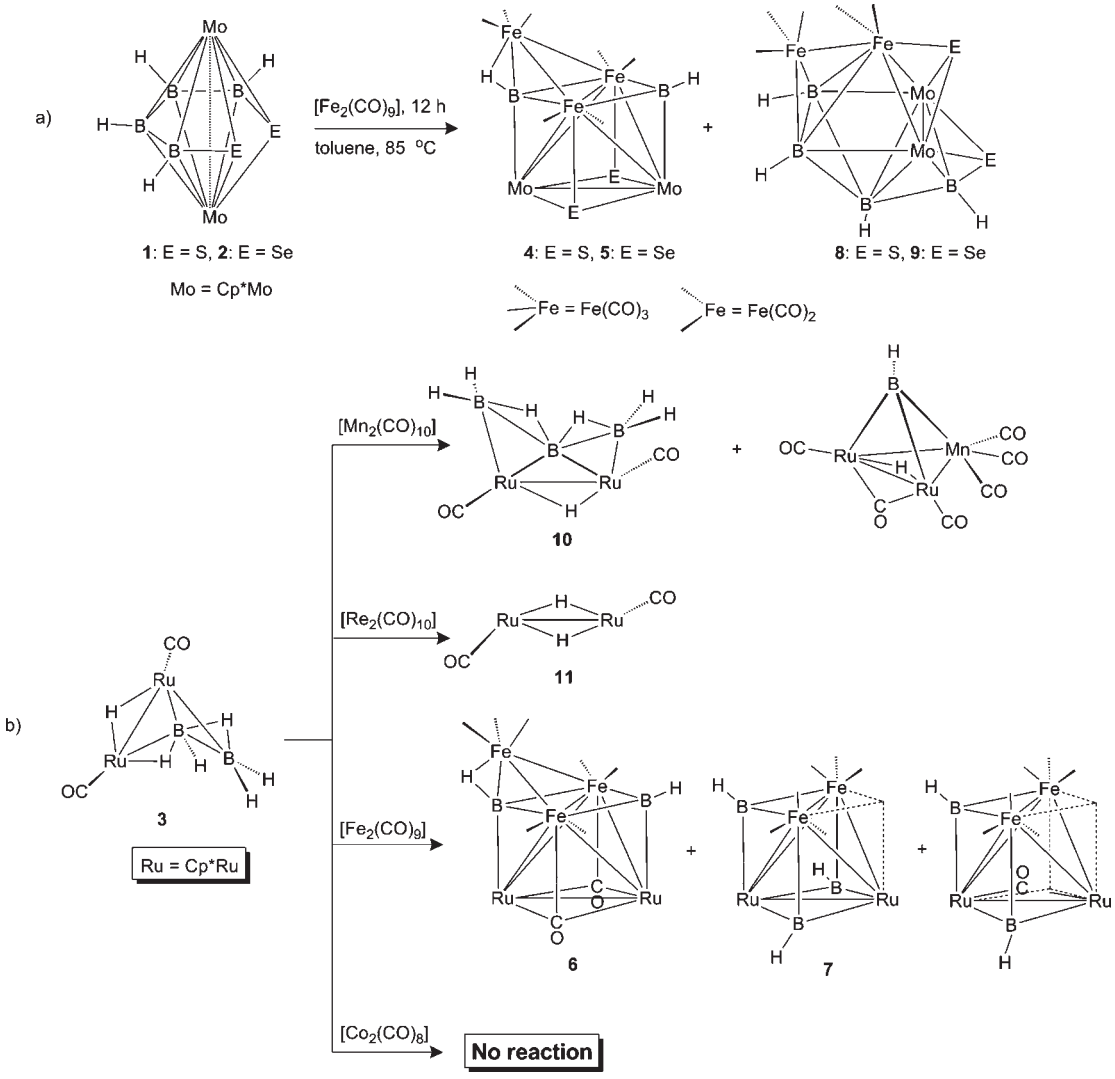

the selenium analogue **5**. The overall structure of **5** is interesting and can be viewed as a cubane shape made of two Mo, two Fe, two Se, and two B atoms and its "cap", a third iron atom, is attached to one of the B−Fe−Fe faces of the cube.

The cubane-type sulfido clusters have been extensively investigated in the chemistry of metal sulfido clusters;[15] in contrast the corresponding selenido derivatives have received little interest, the only structurally characterized examples being the Mo, Sn, and Pd derivatives with $[M_3M'Se_4]$ single cube structure.[16] Compound **5** is the first heterobimetallic selenido cuboidal cluster containing a boride unit (B2) as one of the vertices. The boron atom (B2) lies within an open $MoFe_3$ skeleton which can be described as an open butterfly framework. In **5**, the unique boron atom (B2) lies 0.318 Å above the $Mo_{wing}-Fe_{wing}$ (i.e., Mo(2)−Fe(2)) axis. The internal dihedral angle of the $MoFe_3$ butterfly is 114°, which corresponds well with the value observed for $[HFe_4(CO)_{12}BH_2]$ (114°)[17] and for a four-atom butterfly cluster (109°) derived from an octahedron.[18]

The Mo1−Mo2 bond length of 2.9216(3) Å is in the range observed for a bond order of one but slightly (0.08 Å) longer than the corresponding distances in $[Mo_3CuSe_4Cl_4(dmpe)_3]PF_6$ (dmpe = 1,2-bis(dimethylphosphino)ethane).[16c] The Fe1−Fe3 distance is 2.5220(4) Å, which is 0.2 Å shorter than those observed in single and double-cubane clusters; while the mean Mo−Fe distances of 2.792 Å is not unusual.[19] *Exo*-bonded to the cubane at the B2−Fe1−Fe3 face is the third iron atom (Fe2) with a long Fe−Fe distance of 2.632 Å and the short $Fe-B_{boride}$ bond distance of 2.026(3) Å. The average Mo−Se distance of **5** (2.439 Å) is significantly shorter than that of diselenamolybdaboranes **2** (2.585 Å).

The spectroscopic data of **5** are fully in accord with the solid-state structure, and no evidence of fluxional behavior is observed. The ^{11}B NMR of **4** and **5** rationalize the presence of two boron resonances in the ratio of 1:1. The ^{11}B resonances at δ 143.4 and 144.1 ppm of **4** and **5**, respectively, lie in the range typical of a metal rich boride cluster.[20] In addition to the resonances of the BH proton, the ^1H NMR spectrum also reveals two equivalents of Cp* ligands, indicating two different Mo environments. The ^{13}C NMR spectra contain signals attributable to the two types of Cp* ligands and the $Fe(CO)_3$ fragment. The ^{77}Se NMR spectra of **5** displayed single resonance at δ 995 ppm for the bridged μ_3-Se atoms. The parent ion of **4** and **5** in the mass spectrum fragments by the sequential loss of seven CO molecules, and the molecular mass corresponds to $Cp^*_2Mo_2B_2H_2S_2Fe_3(CO)_7$ and

dx.doi.org/10.1021/ic200802c |*Inorg. Chem.* 2011, 50, 5824–5832

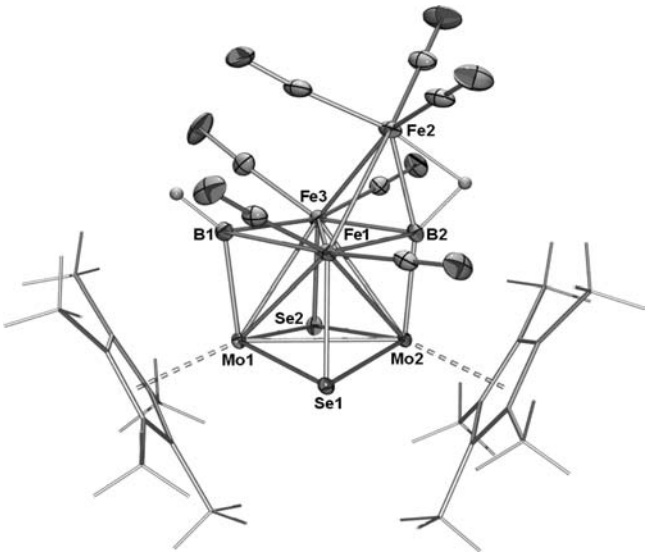

Figure 1. Molecular structure and labeling diagram for **5**. Thermal ellipsoids are shown at the 40% probability level. Selected bond lengths (Å) and angles (deg): Mo1−Mo2 2.9216(3), Mo1−B1 2.115(3), Mo2−B2 2.061(3), Fe1−B1 2.128(3), Fe1−B2 2.056(3), Fe3−B1 2.119(3), Fe3−B2 2.056(3), Mo1−Se2 2.4253(3), Mo2−Se2 2.4544(3), Fe1−Se1 2.4064(4), Fe3−Se2 2.4027(4), Fe1−Fe3 2.5220(4), Fe1−Fe2 2.6294(4), Fe3−Fe2 2.6360(5); B1−Mo1−Se1 101.06(7), Se1−Mo1−Se2 105.829(10), B1−Mo1−Fe1 49.13(7), Mo2−Fe1−Mo1 63.228(9), Mo1−Se1−Mo2 73.575(8), Fe1−Mo2−Fe3 53.582(10).

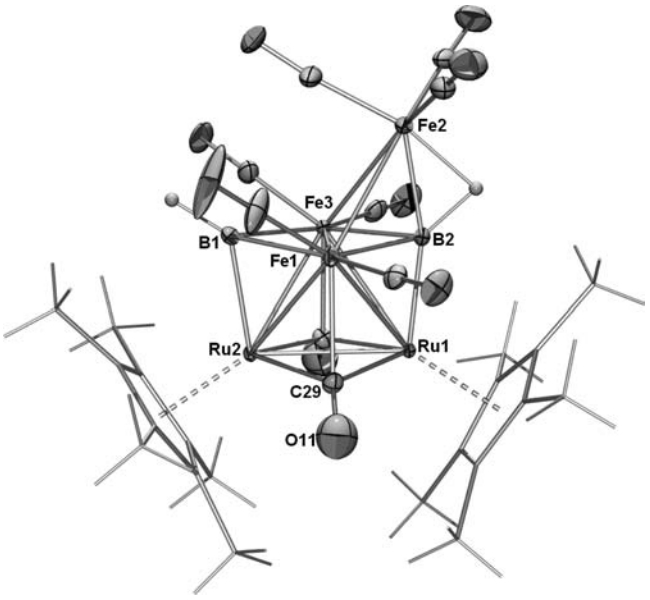

Figure 2. Molecular structure and labeling diagram for **6**. Thermal ellipsoids are shown at the 30% probability level. Selected bond lengths (Å) and angles (deg): Ru1−Ru2 2.7167(4), Ru1−Fe3 2.6663(6), Ru1−Fe1 2.6573(5), Fe2−Fe3 2.6800(7), Fe1−Fe2 2.6735(8), Fe1−Fe3 2.4838(8), Ru2−Fe3 2.64996, Ru2−Fe1 2.6354(6), Ru1−B2 1.985(4), Fe1−B2 2.029(4); B2−Ru1−Fe1 49.27(12), Fe1−Ru1−Fe3 55.623(17), Fe1−Ru1−Ru2 58.721(13), B2−Fe1−B1 105.53(18), B1−Fe1−Fe3 53.41(13), B2−Fe1−Ru2 98.10(12), Ru2−Fe1−Ru1 61.764(13).

$Cp^*_2Mo_2B_2H_2Se_2Fe_3(CO)_7$ respectively. The IR spectrum of compounds **4** and **5** also supports the presence of terminal carbonyl ligands that appeared at 2029, 1978 and 2022, 1976 cm^{-1} respectively.

Mild thermolysis of **3** with $[Fe_2(CO)_9]$ generated **6**, in parallel with the formation of the incomplete cubane cluster $[(\mu_3\text{-BH})_3(Cp^*Ru)_2\{Fe(CO)_3\}_2]$, **7**, and the triply bridged borylene complex $[\{(\mu_3\text{-BH})(Cp^*Ru)Fe(CO)_3\}_2(\mu\text{-CO})]$.[13] The mass spectrum of **6** shows a molecular ion at m/z = 915 corroborating the composition of $C_{29}H_{32}B_2Fe_3Ru_2O_9$. The $^{11}B\{^1H\}$ NMR spectrum displayed two resonances with equal intensities. The peak at δ 128.5 ppm has been assigned to the borylene boron atom, and the significantly deshielded resonance at δ 158.5 ppm has been assigned to the boride boron which implies a greater degree of boron−metal interaction. The ^1H NMR spectra showed one broad signal at lowest field for the terminal BH proton, two sets of distinct chemical shifts for the two Cp* ligands at δ 2.17 and 1.84 ppm, and a singlet at higher field for the Fe−H−B proton at δ −8.48 ppm. The infrared spectrum of **6** shows two strong bands at 2029 and 1978 cm^{-1}, assigned to the CO stretching modes of the Fe(CO) group and a band at 1730 cm^{-1} for the bridging carbonyl stretching frequency.

A single crystal suitable for an X-ray diffraction study could be obtained from a solution of **6** in hexane by slow evaporation of the solvent. The molecular structure and relevant bond lengths and angles are displayed in Figure 2. The structure of **6** adopts cubane-type geometry with four metal atoms at the corners of a tetrahedron with two CO, one BH, and one boride unit capping each face of the tetrahedron. In addition, one of the Fe_2B faces of the cubane is capped by a $Fe(CO)_3$ fragment. The coordination sphere of the Ru atoms is completed by Cp* ligands, and each iron atom has terminally bonded CO ligands. Furthermore, the packing of the unit cell of **6** shows an intermolecular CH--O distance of 2.482 Å, which is shorter than the normal van der Waals H···O separation of 2.6 Å. This may possibly reflect weak hydrogen bonding between the methyl hydrogen of Cp* and the terminal carbonyl oxygen.[21]

The metal−metal distances, 2.7167(4) Å (Ru−Ru), 2.657(9) Å (Ru−Fe), and 2.4838(8) Å (Fe−Fe), are all consistent with single bonds between the metal atoms. All M−M−M angles in a regular tetrahedron are 60°, and the observed angles in **6** are very close to this ideal value. The deviations are a consequence of the shorter Fe−Fe and Ru−Fe distances relative to the Ru−Ru distance. The average triply bridging M−CO (M = Ru, Fe) bond length of 2.088 Å compares favorably with the average value of 2.059 Å observed for the similar triply bridging carbonyl ligand in $[(Cp^*Ru)_3(\mu_3\text{-CO})Co(CO)_2B_3H_3]$.[22] In contrast, the Fe−CO distances for the terminal carbonyl ligands in **6** has an average value of 1.779 Å. This latter value emphasizes that a significant M−CO bond lengthening of approximately 0.25−0.30 Å occurs when a terminal carbonyl ligand bonded to only one metal atom formally transmutes into a ligand symmetrically coordinated to three metal atoms.

Primarily the overall shape of the cubane cluster remains unchanged while the M−M distances reflect changes in cluster electronic structure accompanying the addition and loss of electrons.[23] Earlier, Kennedy in his review[24] described $[(CpNi)_4B_4H_4]$[25] and $[(CpCo)_4B_4H_4]$[26] as 68 and 64-electron clusters, with two and four metal−metal bonds. Further, he suggested that the putative $[(CpFe)_4B_4H_4]$ cluster with 60 electrons should exhibit a cubane structure with six Fe−Fe bonds and a fully bonded metal tetrahedron. The metallaborane that connects these clusters is 60 cluster valence electrons (cve)

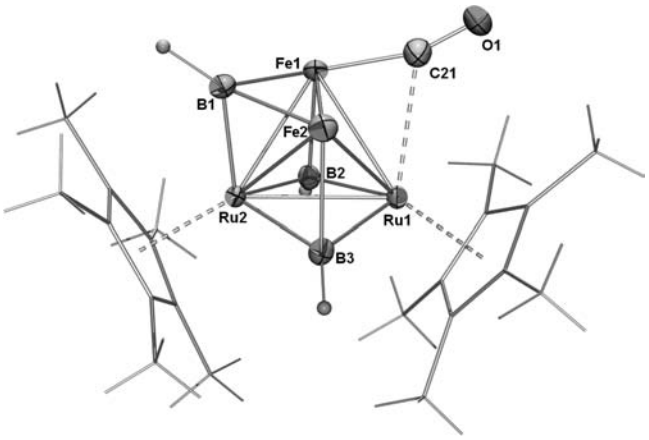

Figure 3. Molecular structure and labeling diagram for **7**. Thermal ellipsoids are shown at the 30% probability level. Terminal carbonyl ligands are excluded for clarity. Selected bond lengths (Å) and angles (deg): Ru1−Ru2 2.7477(3), Ru1−Fe1 2.6088(4), Ru1−Fe2 2.6687(4), Fe1−Fe2 2.6204(5), Ru2−Fe1 2.6155(4), Ru2−Fe2 2.6232(4), Ru2−B1 2.022(3), Fe1−B1 2.078(3), Fe2−B1 2.096(3); Ru2−B1−Fe1 79.27(10), Ru1−Fe1−Fe2 61.375(12), Ru2−Fe1−Fe2 60.132(12), Fe1−Fe2−Ru2 59.842(12).

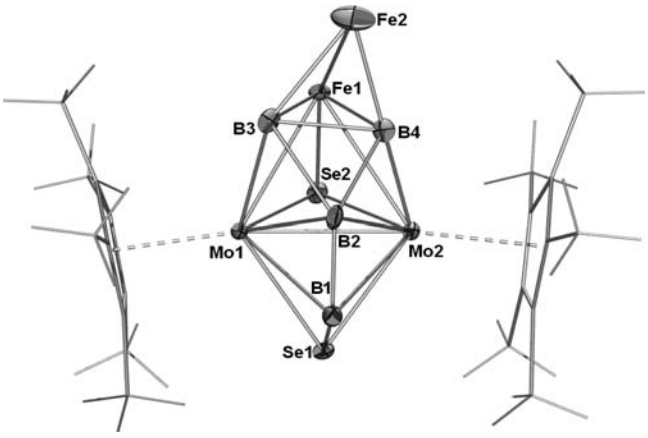

Figure 4. Molecular structure and labeling diagram for **9**. Thermal ellipsoids are shown at the 30% probability level. Terminal carbonyl ligands are excluded for clarity. Selected bond lengths (Å) and angles (deg): Mo1−Mo2 2.7437(16), Mo1−Se1 2.5391(16), Mo1−B1 2.426(16), Fe1−Se2 2.296(2), Fe1−B4 2.085(16), Fe2−B3 2.149(16), Fe1−Fe2 2.634(3), B1−B2 1.71(2), B2−B4 1.79(2), B1−Se1 2.02(2); Mo1−Se1−Mo2 65.46(5), Mo1−B1−Mo2 69.0(4), Mo1−Fe1−Mo2 58.43(5).

$[(Cp^*Ru)_3(\mu_3\text{-}CO)Co(CO)_2B_3H_3]$, a cubane geometry with six M−M bonds.[22] Compounds **4**−**6**, presented in this report, are also 60 cve tetrametal metallaboranes, which can be compared to those discussed above. In fact, the first member (and parent) of this particular class of cubane-like molecules, that is, $[Cp_4Fe_4(\mu_3\text{-}CO)_4]$, also represents a 60 cve cluster with six M−M bonds.

Compound **7** was isolated in 5% yield as a red brown solid. The atom connectivity within the compounds was persuasively determined by performing a single-crystal X-ray diffraction study of **7** (Figure 3). The $Ru_2Fe_2B_3$ core in **7** appears to be the incomplete cubane-type;[28] it consists of a metal−metal bonded Ru_2Fe_2 tetrahedron, in which each Ru atoms bound to a Cp* ligand and Fe atoms bound to carbonyl ligands. The three triangular faces Ru1−Ru2−Fe1, Ru1−Ru2−Fe2, and Ru2−Fe1−Fe2 are capped by a borylene ligand (BH) in a μ_3 fashion; thereby generating a overall tricapped tetrahedron structure **7**. A formal electron count[1] for **7** is in agreement with the metallaborane, $[(Cp^*Re)_2B_4H_8]$,[29] that is, six skeletal electron pair (sep) appropriate for tetrahedral geometry.

The interatomic Ru1−Ru2 distance of 2.7477(3) Å indicates the existence of a single bond between the ruthenium atoms; however, it is slightly longer than observed in **6**. The average B−Ru distance of 2.054 Å lies in the range of those reported for the transition metal borylene complexes.[30] In **7**, one of the carbonyl groups covalently linked to iron (Fe1) interacts with the ruthenium (Ru1) center in a semi bridged fashion (Ru−Fe−CO 66.6°).[13] The average dihedral angle between the plane of B2−Fe1−Fe2−B3 atoms relative to the Cp* ligands is 146.1°, whereas the tilt of the plane of two Cp* ligands is 112.2°.

The ^{1}H and ^{11}B NMR spectra are consistent with the solid-state X-ray structure of **7**, which rationalizes the presence of two boron environments in ratio of 2:1 at δ 126.2 and 92.9 ppm. Furthermore, the ^{1}H NMR spectrum reveals the presence of two Cp* resonances and two terminal B−H protons in the ratio of 2:1. The ^{13}C NMR spectrum indicates the presence of carbonyl ligands that appeared at δ 212.5 and 210.9 ppm. The parent ion of **7** in the mass spectrum fragments by the sequential loss of six CO molecules, and the molecular mass corresponds to $Cp^*_2Ru_2Fe_2(CO)_6B_3H_3$. The IR spectrum shows two terminal carbonyl frequencies at 2009 and 1969 cm^{-1}, and the band at 2489 cm^{-1} is due to the terminal B−H stretches.

Fused Clusters 8 and 9. Compounds **8** and **9** were isolated in 11% and 22% yield as green solids. Unfortunately, all of our efforts to grow single crystals of **8** resulted in weakly diffracting material, and no data sets of sufficient quality for resolution of the molecule were obtained. However, the structure of **8** was confirmed by comparing its spectroscopic data with that of the selenium analogue **9**. Single crystals suitable for X-ray diffraction analysis of **9** were obtained from a hexane solution at −10 °C, thus allowing for the structural characterization of cluster **9**. Compound **9** crystallizes in the triclinic system with a space group $P\bar{1}$. It contains six independent molecules in the asymmetric unit. A solid-state structure of one of the six independent molecules of **9** is shown in Figure 4. The sides *a* and *b* are nearly equal, and the γ angle is 119°. Although it was felt that the crystal suffered from some pseudomerohedral twinning, the exact twin relationship can not be found. The higher residual factor (0.1280) and the unaccountable difference electron density might have been caused by twinning.

The observed geometry of **9** can be viewed as a fused cluster, in which a bicapped octahedron $\{Mo_2Fe_2B_3Se\}$ unit fused with a trigonal bipyramidal $\{Mo_2B_2Se\}$ unit with three atoms held common between the two subclusters. An alternative interpretation of the structure of **9** as a tricapped octahedron, with Mo1, Mo2, B2, B3, B4, and Fe1 occupying the vertices of the core octahedron, in which the faces Mo1−Mo2−Fe1, B3−B4−Fe1, and Mo1−Mo2−B2 are capped by Se2, Fe2, and B1, respectively. The resulting Mo1−Mo2−B1 face in turn is capped by the Se1 atom; thus, cluster **9** may be considered as a tetracapped octahedron. On the basis of the capping principle, the skeletal electron count is determined by the central polyhedron, that is, the $Mo_2Fe_1B_3$ octahedron, and is seven sep. Formally, the μ_3-E (E = S and Se) group contributes four electrons; hence for **8** and **9**, eight sep are available and the observed structures do not obey

dx.doi.org/10.1021/ic200802c |*Inorg. Chem.* 2011, 50, 5824–5832

the counting rules.[1] Although the bicapped octahedral geometry is well-known in metallaborane chemistry,[31] clusters **8** and **9** provide the unique example of a tetracapped octahedral core.

The Mo−Mo bond length of **9** (2.7437(16) Å) is somewhat longer than that found in **2** (2.665(2) Å). The Mo−Fe distances (2.8400(19) and 2.781(2) Å) are consistent with the presence of a single bond and markedly shorter than $[(Cp^*Mo)_2B_5H_9Fe(CO)_3]$.[31a] The Fe−Fe bond distance is within the expected range (2.634 Å). The Mo−B bond lengths show variation within the cluster. Of the direct Mo−B linkages, those to B1 are somewhat longer (2.426(16) and 2.420(17) Å), reflecting a weaker Mo−B interaction. Although the crystal structure of **9** does not display the BH hydrogens, which are assigned using $^1H\{^{11}B\}$ NMR spectroscopy.

The spectroscopic data for **9** in solution also support the solid state structure. Mass spectrometry analysis of **8** and **9** is consistent with a compound of the formulation $Cp^*_2Mo_2B_4H_4S_2Fe_2(CO)_5$ and $Cp^*_2Mo_2B_4H_4Se_2Fe_2(CO)_5$, respectively, and the parent ion shows the sequential loss of five CO molecules. The ^{11}B NMR spectrum of **8** and **9** shows three types of boron environments in the ratio of 2:1:1. The low field ^{11}B chemical shifts of δ 75.1 (**8**) and 74.2 ppm (**9**) may be assigned to the boron that is bonded to three metals. The high field ^{11}B resonances at δ 5.2 (**8**) and 11.6 ppm (**9**) can be assigned to boron bonded to the sulfur and selenium atom, respectively. Furthermore, the ^1H and ^{13}C NMR spectra imply one Cp* ligand, and three distinct BH terminal groups (2:1:1). Terminal BH and CO stretching frequencies are observed in the IR spectrum, and the presence of the latter is confirmed by the ^{13}C NMR spectrum. The ^{77}Se NMR spectra of **9** displayed two resonances at δ 894 and 578 ppm for the bridged μ_3-Se atoms.

Reactivity of 3 toward Group 7 and 9 Metal Carbonyls. In an ongoing effort to access higher order clusters, the reactivity of **3** with other metal fragment sources have been examined. The reactions of **3** with $[Cp^*Re(CO)_3]$ and $[Co_2(CO)_8]$ led to decomposition of the starting material, whereas $[Mn_2(CO)_{10}]$ was found accompanied of a compound identified spectroscopically as *arachno*-$[(Cp^*RuCO)_2B_3H_7]$, **10**, along with the formation of a bridged borylene complex $[(\mu_3\text{-BH})(Cp^*RuCO)_2(\mu\text{-H})(\mu\text{-CO})\{Mn(CO)_3\}]$.[13] Mild thermolysis of **3** with $[Re_2(CO)_{10}]$, on the other hand, produces only the nonboron-containing bridged hydride complex $[Cp^*Ru(CO)(\mu\text{-H})]_2$, **11**.

The FAB mass analysis of **10** gives a molecular ion peak corresponding to $[\{Cp^*Ru\}_2(CO)_2B_3H_7]$, and the presence of terminal metal-bound CO ligands is evident in the IR spectrum. The ^{11}B spectrum exhibits two signals of area 1:2 (δ = 54.5 and −9.7 ppm). A peak at the lower field was assigned to the boron atom that bridges the two ruthenium metals. In addition to the resonances due to the BH proton, the ^1H NMR spectrum reveals a signal at δ 1.81 ppm for the Cp* protons, indicating identical Ru environments and the presence of B−H−B and Ru−H−Ru protons, each appearing at δ −1.54 and −18.19 ppm of intensity 2:1. Consistent with this observation, the ^{13}C NMR spectrum also shows one Cp* signal and the signal due to carbonyl groups. The variable-temperature ^1H and ^{13}C NMR experiments demonstrated that compound **10** is not fluxional.

After recrystallization in hexane, **10** was isolated as air- and moisture-sensitive yellow crystals. The molecular structure of **10**, shown in Figure 5, is determined by single-crystal X-ray diffraction studies. The framework structure of **10** is predicted by the electron counting rules to be an eight sep, five-vertex *arachno* cluster. In terms of structure, consider the ancillary ligands first; the Cp* ligands and the carbonyl groups are arranged in a transoid fashion. As shown in Figure 5, opening a basal-apical edge of a *nido* square pyramidal cluster generates the observed geometry. *Arachno*-**10** is a structural isomer of $[\{Cp^*Ru\}_2(CO)_2B_3H_7]$,[32] **I**, reported earlier by Fehlner (Chart 1). The bridging hydrogen along the Ru1−Ru2 edge has not been positioned by X-ray diffraction studies; however, its connectivity with Ru1 and Ru2 has been assertively determined by ^1H NMR.

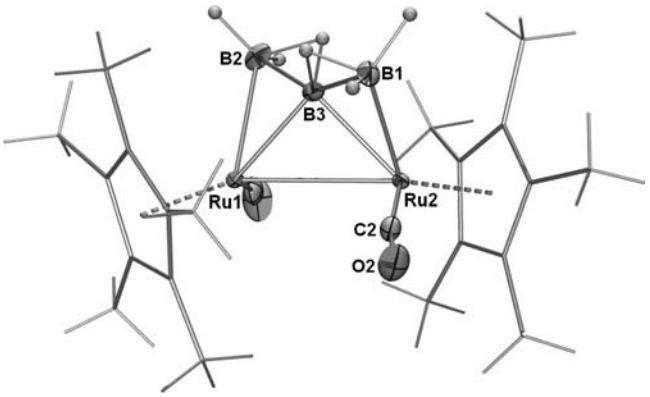

Figure 5. Molecular structure and labeling diagram for **10**. Thermal ellipsoids are shown at the 30% probability level. Selected bond lengths (Å) and angles (deg): Ru1−Ru2 2.9386(8), Ru1−B2 2.302(9), Ru2−B3 2.118(9), B1−B3 1.758(13), B2−B3 1.761(13); B2−Ru1−Ru2 84.6(2), B3−Ru2−B1 46.8(4), B1−Ru2−Ru1 85.5(3), B3−Ru2−Ru1 46.4(2).

Chart 1. Structural Comparison of 10 and $[\{Cp^*Ru\}_2(CO)_2B_3H_7]$, I

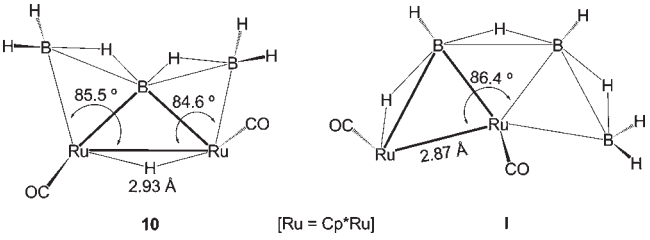

In cluster **10** the interatomic distance between Ru1 and Ru2 (2.9386(8) Å) is near the longer limit of reported Ru−Ru single bond distances. This difference is consistent with the presence of a bridging hydrogen atom at the Ru1−Ru2 edge, resulting in a longer Ru−Ru interaction. The average bond length of Ru2 and the boron atom at the bridging position, B3 (2.124 Å), is substantially shorter than that Ru2−B1 (2.293(10) Å) and Ru1−B2 (2.302(9) Å). The dihedral angle between the three-membered rings of Ru2−Ru1−B3 and B3−Ru2−B1 is 138.3°. This value is slightly wider than the corresponding angle in *arachno*-B_4H_{10} (125.5° by electron diffraction;[33] 117.4° by electron diffraction and microwave spectroscopy) and reported *arachno*-dimetallaboranes.[34]

The number of metal, boron, and hydrogen atoms in **10** and **I** remains the same, and considering the close similarity of the chemical shifts indicates that the structures of **10** and **I** are closely related. **I** is shown to convert into a second isomeric form of similar stability. Although **10** and **I** have the same metal−metal,

boron−boron, and metal−boron connectivities, there are some significant differences in the arrangement of hydrogen atoms and the structural metrics. Selected comparisons are given in Chart 1. For instance, the major differences between **10** and **I** can be appreciated by looking at the Ru−Ru bond distance and the atoms in the M−M−B plane as shown in Chart 1. In going from **10** to **I**, the metal−metal and metal−boron distances shorten and the M−M−B angles open. Furthermore, the environments of the boron atoms are slightly changed from those in **I**, and the difference is the metal to which the BH_2 group is attached and their hydrogen atoms. In the case of **I** the low-field ^{11}B resonance is coupled to the high-field B−H−Ru proton and one terminal proton. In contrast, the low field ^{11}B resonance of **10** coupled to the high-field B−H−B protons only.

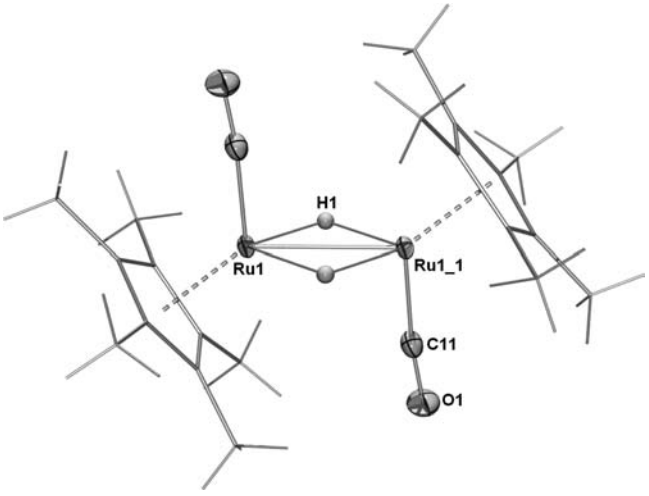

Figure 6. Molecular structure and labeling diagram for **11**. Thermal ellipsoids are shown at the 40% probability level. Selected bond lengths (Å) and angles (deg): Ru1−Ru1_1 2.6920(3), Ru1−H1 1.806(19); O1−C11−Ru1 173.75(16), C11−Ru1−H1 95.2(6), C11−Ru1−Ru1_1 94.52(5).

The pathway for the formation of **10** from **3** is of interest. A plausible reaction stochiometry is shown in eq 1. As loss of BH_3 and H_2 is a common feature of borane, as well as metallaborane cluster chemistries,[35] the formation of **10** is most simply viewed as a metallaborane combination followed by $[HMn(CO)_5]$ loss.

$$2[(Cp^*RuCO)_2B_2H_6] + [Mn_2(CO)_{10}] \xrightarrow{\Delta} \underset{\mathbf{10}}{[(Cp^*RuCO)_2B_3H_7]} + [(Cp^*RuCO)_2BH_2\{Mn(CO)_4\}] + [HMn(CO)_5] + CO + H_2 \quad (1)$$

Although the objective of the thermolysis of **3** with $[Re_2(CO)_{10}]$ was to generate an analogue of the bridged borylene complex $[(\mu_3\text{-BH})(Cp^*RuCO)_2(\mu\text{-H})(\mu\text{-CO})\{Mn(CO)_3\}]$, it led to the isolation of nonboron compound **11**. Compound **11** has been isolated and spectroscopically characterized by Forrow and Knox;[36] however, no detailed structural insights were available. In this report we describe the isolation (under different reaction conditions) and structural characterization of **11**. From the mass spectral analysis combined with the ^1H NMR spectrum, **11** is formulated as $[Cp^*Ru(CO)(H)]_2$. A single-crystal X-ray diffraction study has been carried out on **11** with the results shown in Figure 6. The osmium analogue of **11** had been synthesized and structurally characterized previously.[37] The structure of **11** consists of a diruthenium unit bridged by a pair of μ-H atoms. In addition, each Ru atom has a Cp* ligand and a terminally bound carbonyl group attached to it. The terminal carbonyl groups and Cp* ligands have an anti orientation with respect to

Table 1. Crystallographic Data and Structure Refinement Information for 5−7 and 9−11

	5	6	7	9	10	11
empirical formula	$C_{27}H_{32}B_2Fe_3Mo_2O_7Se_2$	$C_{29}H_{32}B_2Fe_3Ru_2O_9$	$C_{26}H_{33}B_3Fe_2Ru_2O_6$	$C_{63}H_{76}B_8Fe_4Mo_4O_{11}Se_4$	$C_{22}H_{37}B_3O_2Ru_2$	$C_{22}H_{30}O_2Ru_2$
formula weight	1007.50	915.86	787.79	2018.72	568.09	528.60
crystal system	monoclinic	triclinic	monoclinic	triclinic	monoclinic	monoclinic
space group	$P2_1/c$	$P\bar{1}$	$P2_1$	$P\bar{1}$	$P2_1/n$	$P2_1/n$
a (Å)	12.2619(4)	10.3081(4)	9.3791(8)	18.0715(9)	8.3363(4)	7.2377(3)
b (Å)	13.3712(3)	10.8988(5)	14.9670(14)	18.3109(9)	36.354(2)	15.2598(6)
c (Å)	21.2481(6)	16.0185(7)	10.9142(9)	41.907(2)	9.1085(4)	10.1424(4)
α (deg)	90	74.054(4)	90.00	92.939(3)	90	90
β (deg)	106.675(3)	81.082(3)	106.910(4)	97.194(2)	116.469(6)	107.4460(10)
γ (deg)	90	67.255(4)	90.00	119.025(2)	90	90
V (Å^3)	3337.26(16)	1593.39(12)	1465.9(2)	11929.4(11)	2471.1(2)	1068.66(7)
Z	4	2	2	6	4	2
D_{calc} (g/cm^3)	2.005	1.909	1.785	1.686	1.527	1.643
F (000)	1960	908	784	5940	1152	532
μ (mm^{-1})	4.226	2.311	2.019	3.198	1.237	1.425
θ range (deg)	3.37- 25.00	3.32−25.00	2.27−24.99	0.99−25.00	3.36−25.00	2.49−28.49
no. of refins collected	25265	10911	27674	135275	16928	7722
no. of unique refins [$I > 2\sigma(I)$]	5867	5578	5135	135275	4335	2651
goodness-of-fit on F^2	1.027	1.045	1.036	1.098	1.350	1.262
final R indices [$I > 2\theta(I)$]	R1 = 0.0172	R1 = 0.0257	R1 = 0.0136	R1 = 0.1280	R1 = 0.0675	R1 = 0.0182
	wR2 = 0.0416	wR2 = 0.0750	wR2 = 0.0341	wR2 = 0.3117	wR2 = 0.1057	wR2 = 0.0499
R indices (all data)	R1 = 0.0205	R1 = 0.0310	R1 = 0.0140	R1 = 0.1839	R1 = 0.0779	R1 = 0.0217
	wR2 = 0.0423	wR2 = 0.0763	wR2 = 0.0343	wR2 = 0.3417	wR2 = 0.1083	wR2 = 0.0520

dx.doi.org/10.1021/ic200802c |*Inorg. Chem.* 2011, 50, 5824–5832

the Ru−Ru bond. The Ru−Ru distance of 2.6920(3) Å in **11** is much shorter than observed in **3** (2.9258(10) Å) and longer than the hydrido carbonyl complex [(Cp*Ru(μ-H)$_2$(μ-CO)RuCp*] (2.444(1) Å).[38] The Ru−Ru distance in **11** is considerably longer than the Ru═Ru distance of 2.26−2.29 Å, observed in tetracarboxylate ruthenium(II) dimers and other related species.[39] The terminal CO ligands are almost linear, with a Ru−C−O angle of 173.7°. The Ru(μ-H)$_2$Ru core of **11** is planar, and the dihedral angle between the plane of the central core relative to the Cp* ligand is 127.2°.

CONCLUSION

From the results described in this article, it can be concluded that reaction of group 6 or 8 metallaboranes or their derivatives with metal carbonyl fragments constitute a useful route to heterometallaborane clusters. Compounds **8** and **9** represent a novel class of hybrid clusters, in which a [Mo_2B_2Se] trigonal bipyramid has been fused to a [$Mo_2Fe_2B_3Se$] bicapped octahedron subcluster. Further, as demonstrated in this article, the difference in reactivity pattern of the different metal carbonyls with [(Cp*RuCO)$_2B_2H_6$], **3**, is also reflected in the observed product distribution.

EXPERIMENTAL SECTION

General Procedures and Instrumentation. All the operations were conducted under an Ar/N_2 atmosphere using standard Schlenk techniques or glovebox. Solvents were distilled prior to use under Argon. [$Co_2(CO)_8$], [$Mn_2(CO)_{10}$], [$Re_2(CO)_{10}$], [$Fe_2(CO)_9$] (Aldrich) and [Cp*Re$(CO)_3$] (Strem) were used as received. Compounds **1**−**3** were prepared according to literature methods.[12,13] The external reference [$Bu_4N(B_3H_8)$] for the ^{11}B NMR was synthesized with the literature method.[40] Thin layer chromatography was carried on 250 mm dia aluminum supported silica gel TLC plates (MERCK TLC Plates). NMR spectra were recorded on a 400 and 500 MHz Bruker FT-NMR spectrometer. Residual solvent protons were used as reference (δ, ppm, $CDCl_3$, 7.26), while a sealed tube containing [$Bu_4N(B_3H_8)$] in [D_6]benzene (δ_B, ppm, −30.07) was used as an external reference for the ^{11}B NMR. Infrared spectra were recorded on a Nicolet 6700 FT spectrometer. Microanalyses for C, H, and N were performed on Perkin Elmer Instruments series II model 2400. Mass spectra were obtained on a Jeol SX 102/Da-600 mass spectrometer with argon/xenon (6kv, 10 mÅ) as FAB gas.

Synthesis of 4−9. In a typical reaction, compound **1** (0.07 g, 0.12 mmol) in toluene (15 mL) was stirred with 4 equiv of [$Fe_2(CO)_9$] (0.17 g, 0.48 mmol) for 12 h at 85 °C. The solvent was removed in vacuo, the residue was extracted in hexane, and passed through Celite. The filtrate was concentrated and kept at −40 °C to remove [$Fe_3(CO)_{12}$]. The mother liquor was concentrated, and the residue was chromatographed on silica gel TLC plates. Elution with a hexane/CH_2Cl_2 (9:1) mixture yielded **4** (0.005 g, 4%) and **8** (0.011 g, 11%). The isolated yield of the Se analogue **5** and **9** from **2** were 16% (0.017 g) and 22% (0.021 g), respectively. Further, in a similar fashion, reaction of **3** (0.075 g, 0.13 mmol) in hexane at 65 °C provided **6** (0.02 g, 16%), along with the formation of **7** (0.005 g, 5%) and [{(μ_3-BH)(Cp*Ru)Fe$(CO)_3$}$_2$-(μ-CO)] (0.03 g, 27%).

4: ^{11}B NMR (25 °C, 128 MHz, $CDCl_3$,): δ 143.4 (br, 1B), 107.2 ppm (br, 1B). ^{1}H NMR (25 °C, 400 MHz, $CDCl_3$): δ 9.95 (partially collapsed quartet (pcq), 1BH$_t$), 1.74 (s, 15H, 1Cp*), 1.68 (s, 15H, 1Cp*), −7.86 ppm (s, 1H, Fe−H−B). ^{13}C NMR (25 °C, 100 MHz, $CDCl_3$): δ 215.5, 203.4 (s, CO), 108.6, 105.9 (s, C_5Me_5), 13.1, 12.8 ppm (s, C_5Me_5). IR (hexane) ν/cm^{-1}: 2496w (BH$_t$), 2029, 1978 cm^{-1} (CO). MS (FAB) P$^+$(max): m/z (%) 913.

5: ^{11}B NMR (25 °C, 128 MHz, $CDCl_3$): δ 144.1 (br, 1B), 108.1 ppm (br, 1B). ^{1}H NMR (25 °C, 400 MHz, $CDCl_3$): δ 9.98 (pcq, 1BH$_t$), 1.73 (s, 15H, 1Cp*), 1.66 (s, 15H, 1Cp*), −7.78 ppm (s, 1H, Fe−H−B). ^{13}C NMR (25 °C, 100 MHz, $CDCl_3$): δ 216.2, 203.8 (s, CO), 112.9, 104.7 (s, C_5Me_5), 12.8, 12.3 ppm (s, C_5Me_5). ^{77}Se NMR (25 °C, 95 MHz, $CDCl_3$): δ 995 ppm (s, 2Se). IR (hexane) ν/cm^{-1}: 2449w (BH$_t$), 2022, 1976 cm^{-1} (CO). MS (FAB) P$^+$(max): m/z (%) 1007. Elem anal. Calcd for $C_{27}H_{32}B_2Fe_3Mo_2O_7Se_2$: C, 32.19; H, 3.20. Found: C, 33.02; H, 3.36.

6: ^{11}B NMR (25 °C, 128 MHz, $CDCl_3$): δ 158.5 (br, 1B), 128.5 ppm (br, 1B). ^{1}H NMR (25 °C, 400 MHz, $CDCl_3$): δ 8.48 (pcq, 1BH$_t$), 2.17 (s, 15H, 1Cp*), 1.84 (s, 15H, 1Cp*), −8.48 ppm (s, 1H, Fe−H−B). ^{13}C NMR (25 °C, 100 MHz, $CDCl_3$): δ 215.5, 209.4 (s, CO), 120.3, 119.9 (s, C_5Me_5), 13.1, 9.0 ppm (s, C_5Me_5). IR (hexane) ν/cm^{-1}: 2465w (BH$_t$), 2029, 1978 (CO), 1730 cm^{-1} (μ_3-CO). MS (FAB) P$^+$(max): m/z (%) 915. Elem anal. Calcd for $C_{29}H_{32}B_2Fe_3Ru_2O_9$: C, 38.03; H, 3.52. Found: C, 39.28; H, 3.72.

7: ^{11}B NMR (25 °C, 128 MHz, $CDCl_3$): δ 126.2 (br, 2B), 92.9 ppm (br, 1B). ^{1}H NMR (25 °C, 400 MHz, $CDCl_3$): δ 8.48 (pcq, 2BH$_t$), 8.15 (pcq, 1BH$_t$) 1.84 (s, 15H, 1Cp*), 1.76 (s, 15H, 1Cp*). ^{13}C NMR (25 °C, 100 MHz, $CDCl_3$): δ 212.5, 210.9 (s, CO), 113.2, 104.1 (s, C_5Me_5), 14.4, 9.7 ppm (s, C_5Me_5). IR (hexane) ν/cm^{-1}: 2489w (BH$_t$), 2009 m, 1969 m (CO) cm^{-1}. MS (FAB) P$^+$(max): m/z (%) 787. Elem anal. Calcd for $C_{26}H_{33}B_3Fe_2Ru_2O_6$: C, 39.63; H, 4.22. Found: C, 38.18; H, 3.92.

8: ^{11}B NMR (25 °C, 128 MHz, $CDCl_3$): δ 75.1 (br, 2B), 61.4 (s, 1B), 5.2 (s, br, 1B). ^{1}H NMR (25 °C, 400 MHz, $CDCl_3$): δ 6.05 (pcq, 2BH$_t$), 1.94 (s, 30H, 2Cp*), −0.26 (pcq, 1BH$_t$), −0.63 (pcq, 1BH$_t$). ^{13}C NMR (25 °C, 100 MHz, $CDCl_3$): δ 217.1, 211.2 (CO), 108.4 (s; C_5Me_5), 12.8 (s; C_5Me_5). IR (hexane) ν/cm^{-1}: 2485w (BH$_t$), 2038 m, 1983 m (CO). MS (FAB) P$^+$(max): m/z (%) 825. Elem anal. Calcd for $C_{25}H_{34}B_4Fe_2Mo_2O_5S_2$: C, 36.37; H, 4.15. Found: C, 36.32; H, 4.12.

9: ^{11}B NMR (25 °C, 128 MHz, $CDCl_3$): δ 74.2 (br, 2B), 58.5 (s, 1B), 11.6 (s, br, 1B). ^{1}H NMR (25 °C, 400 MHz, $CDCl_3$): δ 6.26 (pcq, 2BH$_t$), 1.93 (s, 30H, 2Cp*), 0.62 (pcq, 1BH$_t$), −0.63 (pcq, 1BH$_t$). ^{13}C NMR (25 °C, 100 MHz, $CDCl_3$): δ 218.4, 211.1 (CO), 107.2 (s; C_5Me_5), 13.5 (s; C_5Me_5). ^{77}Se NMR (25 °C, 95 MHz, $CDCl_3$): δ 894 and 578 ppm (s, 2Se). IR (hexane) ν/cm^{-1}: 2474w (BH$_t$), 2039 m, 1981 m (CO). MS (FAB) P$^+$(max): m/z (%) 919. Elem anal. Calcd for $C_{25}H_{34}B_4Fe_2Mo_2O_5Se_2$: C, 32.66; H, 3.72. Found: C, 32.60; H, 3.71.

Synthesis of 10 and 11. A yellow solution of compound **3** (0.075 g, 0.13 mmol) in toluene (15 mL) was stirred at 85 °C in the presence of 3 equiv of [$Mn_2(CO)_{10}$] (0.154 g, 0.39 mmol) for 12 h. All volatiles were removed in vacuo, the residue was extracted into hexane, and passed through Celite. The mother liquor was concentrated, and the residue was chromatographed on silica gel TLC plates. Elution with hexane/CH_2Cl_2 (8:2 v/v) yielded yellow **10** (0.011 g, 14%) and reddish brown bridged borylene [(μ_3-BH)(Cp*RuCO)$_2$(μ-H)(μ-CO){Mn$(CO)_3$}] (0.023 g, 24%). Under similar reaction conditions, [$Re_2(CO)_{10}$] (0.254 g, 0.39 mmol) yielded red **11** (0.03 g, 42%).

Compound **11** has been characterized by comparison of its spectroscopic data with those reported by Knox et al.[36]

10: ^{11}B NMR (25 °C, 128 MHz, $CDCl_3$): δ 54.5 (br, 1B), −9.7 ppm (br, 2B). ^{1}H NMR (25 °C, 400 MHz, $CDCl_3$): δ 2.76 (pcq, 4BH$_t$), 1.81 (s, 30H, 2Cp*), −1.54 ppm (br, 2H, B−H−B), −18.19 ppm (s, 1H, Ru−H−Ru). ^{13}C NMR (25 °C, 100 MHz, $CDCl_3$): δ 210.4 (s, CO), 112.4 (s, C_5Me_5), 10.1 ppm (s, C_5Me_5). IR (hexane) ν/cm^{-1}: 2469w (BH$_t$), 1934 (CO). MS (FAB) P$^+$(max): m/z (%) 568. Elem anal. Calcd for $C_{22}H_{37}B_3Ru_2O_2$: C, 46.51; H, 6.56. Found: C, 45.29; H, 5.91.

X-ray Structure Determination. Crystallographic informations for **5**−**7**, and **9**−**11** are listed in Table 1. Crystal data for **5**, **6**, and **10** were collected and integrated using Oxford Diffraction Xalibur-S CCD system equipped with graphite-monochromated Mo Kα radiation

(λ = 0.71073 Å) radiation at 150 K. The crystal data for **7**, **9**, and **11** were collected and integrated using a Bruker Axs kappa apex2 CCD diffractometer, with graphite monochromated Mo−Kα (λ = 0.71073 Å) radiation at 293, 273, and 173 K respectively. The structures were solved by heavy atom methods using SHELXS-97 or SIR92[41] and refined using SHELXL-97 (Sheldrick, G. M., University of Göttingen).[42,43]

■ ASSOCIATED CONTENT

Supporting Information. The supplementary crystallographic data and X-ray crystallographic files for **5**−**7**, and **9**−**11**. This material is available free of charge via the Internet at http://pubs.acs.org.

■ AUTHOR INFORMATION

Corresponding Author
*E-mail: sghosh@iitm.ac.in.

■ ACKNOWLEDGMENT

Generous support of the Department of Science and Technology, DST (Project No. SR/S1/IC-19/2006), New Delhi, is gratefully acknowledged. K.G. and S.K.B. thank the Council of Scientific and Industrial Research (CSIR) and University Grants Commission (UGC), India, respectively for Research Fellowships. We would also like to thank Mass lab, SAIF, CDRI, Lucknow 226001, India, for FAB mass analysis and SAIF, IIT Madras, for variable temperature NMR facilities.

■ REFERENCES

(1) (a) Wade, K. *Electron Deficient Compounds*; Nelson: London, 1971. (b) Wade, K. *Inorg. Nucl. Chem. Lett.* **1972**, *8*, 559. (c) Mingos, D. M. P. *Nature (London)* **1972**, *236*, 99–102. (d) Wade, K. *New Sci.* **1974**, *62*, 615. (e) Wade, K. *Adv. Inorg. Chem. Radiochem.* **1976**, *18*, 1–66. (f) Mingos, D. M. P. *J. Chem. Soc., Chem. Commun.* **1983**, 706–708. (g) Mingos, D. M. P.; Johnston, R. L. *Struct. Bonding (Berlin)* **1987**, *68*, 29.(h) Mingos, D. M. P.; Wales, D. J. *Introduction to Cluster Chemistry*; Prentice Hall: New York, 1990.

(2) (a) Kennedy, J. D. *Prog. Inorg. Chem.* **1984**, *32*, 519–679. (b) Kennedy, J. D. *Prog. Inorg. Chem.* **1986**, *36*, 211–434.(c) Gilbert, K. B.; Boocock, S. K.; Shore, S. G. In *Comprehensive Organometallic Chemistry*; Wilkinson, G., Abel, E. W., Stone, F. G. A., Eds.; Pergamon: New York, 1982; Part 6, Chapter 41, pp 879−945. (d) Grimes, R. N. In *Comprehensive Organometallic Chemistry*; Wilkinson, G., Abel, E. W., Stone, F. G. A., Eds.; Pergamon: New York, 1982; Part 1, Chapter 5.5, pp 459−453.

(3) Wang, X.; Sabat, M.; Grimes, R. N. *Organometallics* **1995**, *14*, 4668–4675.

(4) Le Guennic, B.; Jiao, H.; Kahlal, S.; Saillard, J.-Y.; Halet, J.-F.; Ghosh, S.; Beatty, A. M.; Rheingold, A. L.; Fehlner, T. P. *J. Am. Chem. Soc.* **2004**, *126*, 3203–3217.

(5) Ghosh, S.; Fehlner, T. P.; Beatty, A. M. *Chem. Commun.* **2005**, 3080–3082.

(6) Lei, X.; Shang, M.; Fehlner, T. P. *Angew. Chem., Int. Ed.* **1999**, *38*, 1986–1989.

(7) Vites, J. C.; Housecroft, C. E.; Eigenbrot, C.; Buhl, M. L.; Long, G. J.; Fehlner, T. P. *J. Am. Chem. Soc.* **1986**, *108*, 3304–3310.

(8) (a) Grebenik, P. D.; Green, M. L. H.; Kelland, M. A.; Leach, J. B.; Mountford, P.; Stringer, G.; Walker, N. M.; Wong, L. L. *J. Chem. Soc., Chem. Commun.* **1988**, 799–801. (b) Grebenik, P. D.; Green, M. L. H.; Leach, J. B.; Walker, N. M. *J. Organomet. Chem.* **1988**, *345*, C13–C16. (c) Grebenik, P. D.; Leach, J. B.; Kelland, M. A.; Green, M. L. H.; Mountford, P. *J. Chem. Soc., Chem. Commun.* **1989**, 1397–1399.

(9) Coffy, T. J.; Medford, G.; Plotkin, J.; Long, G. J.; Shore, S. G. *Organometallics* **1989**, *8*, 2404–2409.

(10) Ting, C.; Messerle, L. *J. Am. Chem. Soc.* **1989**, *111*, 3449–3450.

(11) Meng, X.; Bandyopadhyay, A. K.; Fehlner, T. P.; Grevels, F.-W. *J. Organomet. Chem.* **1990**, *394*, 15–27.

(12) Sahoo, S.; Mobin, S. M.; Ghosh, S. *J. Organomet. Chem.* **2010**, *695*, 945–949.

(13) Geetharani, K.; Bose, S. K.; Varghese, B.; Ghosh, S. *Chem.—Eur. J.* **2010**, *16*, 11357–11366.

(14) Geetharani, K.; Bose, S. K.; Sahoo, S.; Ghosh, S. *Angew. Chem., Int. Ed.* **2011**, *50*, 3908–3911.

(15) *Transition Metal Sulfur Chemistry*; Stiefel, E. I., Matsumoto, K., Eds.; American Chemical Society: Washington, DC, 1995.

(16) (a) Fedin, V. P.; Sokolov, M. N.; Virovets, A. V.; Podberezskaya, N. V.; Fedorov, V. Y. *Inorg. Chim. Acta* **1998**, *269*, 292–296. (b) Sokolov, M. N.; Dybtsev, D. N.; Virovets, A. V.; Hegetschweiler, K.; Fedin, V. P. *Russ. Chem. Bull.* **2000**, *49*, 1877–1881. (c) Llusar, R.; Uriel, S.; Vicent, C. *J. Chem. Soc., Dalton Trans.* **2001**, 2813–2818.

(17) Wong, K. S.; Scheidt, W. R.; Fehlner, T. P. *J. Am. Chem. Soc.* **1982**, *104*, 1111–1113.

(18) Fehlner, T. P.; Housecroft, C. E.; Scheidt, W. R.; Wong, K. S. *Organometallics* **1983**, *2*, 825–833.

(19) (a) Holm, R. H.; Simhon, E. D. *Molybdenum Enzymes*; Spiro, T., Ed.; Wiley-Interscience: New York, 1985. (b) Zhang, Y.-P.; Bashkin, J. K.; Holm, R. H. *Inorg. Chem.* **1987**, *26*, 694–702.

(20) (a) Housecroft, C. E. *Polyhedron* **1987**, *6*, 1935–1958. (b) Housecroft, C. E. *Coord. Chem. Rev.* **1995**, *143*, 297–330.

(21) Neuman, M. A.; Trin-Toan; Dahl, L. F. *J. Am. Chem. Soc.* **1972**, *94*, 3383–3388.

(22) Lei, X.; Shang, M.; Fehlner, T. P. *Organometallics* **2000**, *19*, 4429–4431.

(23) Fehlner, T. P.; Halet, J.-F.; Saillard, J.-Y. *Molecular Clusters. A Bridge to Solid-State Chemistry*; Cambridge University Press: Cambridge, U.K., 2007.

(24) Kennedy, J. D. *Prog. Inorg. Chem.* **1984**, *34*, 211–434.

(25) Bowser, J. R.; Bonny, A.; Pipal, J. R.; Grimes, R. N. *J. Am. Chem. Soc.* **1979**, *101*, 6229–6236.

(26) Pipal, J. R.; Grimes, R. N. *Inorg. Chem.* **1979**, *18*, 257–263.

(27) (a)King, R. B. *Inorg. Chem.* **1966**, *5*, 2227–2230.

(28) (a) Hernandez-Molina, R.; Sykes, A. G. *Coord. Chem. Rev.* **1999**, *187*, 291–302. (b) Llusar, R.; Uriel, S. *Eur. J. Inorg. Chem.* **2003**, 1271–1290.

(29) Ghosh, S.; Shang, M.; Fehlner, T. P. *J. Organomet. Chem.* **2000**, *614*−*615*, 92–98.

(30) Pierce, G. A.; Vidovic, D.; Kays, D. L.; Coombs, N. D.; Thompson, A. L.; Jemmis, E. D.; De, S.; Aldridge, S. *Organometallics* **2009**, *28*, 2947–2960.

(31) (a) Aldridge, S.; Hashimoto, H.; Kawamura, K.; Shang, M.; Fehlner, T. P. *Inorg. Chem.* **1998**, *37*, 928–940. (b) Bose, S. K.; Ghosh, S.; Noll, B. C.; Halet, J.-F.; Saillard, J.-Y.; Vega, A. *Organometallics* **2007**, *26*, 5377–5385. (c) Bould, J.; Rath, N. P.; Barton, L. *Organometallics* **1995**, *14*, 2119–2122.

(32) DiPasquale, A.; Lei, X.; Fehlner, T. P. *Organometallics* **2001**, *20*, 5044–5049.

(33) Nordman, C. E.; Lipscomb, W. N. *J. Chem. Phys.* **1953**, *21*, 1856–1864.

(34) Hata, M.; Kawano, Y.; Shimoi, M. *Inorg. Chem.* **1998**, *37*, 4482–4483.

(35) Mavunkal, I. J.; Noll, B. C.; Meijboom, R.; Muller, A.; Fehlner, T. P. *Organometallics* **2006**, *25*, 2906–2907.

(36) Forrow, N. J.; Knox, S. A. R. *J. Chem. Soc., Chem. Commun.* **1984**, 679–681.

(37) Hoyano, J. K.; Graham, W. A. G. *J. Am. Chem. Soc.* **1982**, *104*, 3722–3723.

(38) Kang, B.-S.; Koelle, U.; Thewalt, U. *Organometallics* **1991**, *10*, 2569–2573.

(39) Chakravarty, A. R.; Cotton, F. A.; Tocher, D. A. *Inorg. Chem.* **1985**, *24*, 172–177.

(40) Ryschkewitsch, G. E.; Nainan, K. C. *Inorg. Synth.* **1974**, *15*, 113–114.
(41) Altomare, A.; Cascarano, G.; Giacovazzo, C.; Guagliardi, A. *J. Appl. Crystallogr.* **1993**, *26*, 343–350.
(42) Sheldrick, G. M. *SHELXS-97*; University of Göttingen: Göttingen, Germany, 1997.
(43) Sheldrick, G. M. *SHELXS-97*; University of Göttingen: Göttingen, Germany, 1997.